

1 **Supplementary Information**

2

3

4 **Experimental and computational analyses reveal that environmental**
5 **restrictions shape HIV-1 spread in 3D cultures**

6

7 Andrea Imle, Peter Kumberger, Nikolas D. Schnellbacher, Jana Fehr, Paola
8 Carrillo-Bustamante, Janez Ales, Philip Schmidt, Christian Ritter, William J.
9 Godinez, Barbara Müller, Karl Rohr, Fred A. Hamprecht, Ulrich S. Schwarz,
10 Frederik Graw and Oliver T. Fackler

11

12

13

14

15

16 **Supplementary Table 1.:** Model parameters adjusted with pyABC. 14 parameters were
 17 adjusted with pyABC. The best estimate for each parameter was retrieved from the parameters
 18 from pyABC that resulted in the smallest distance between cell motilities from experimental
 19 data and simulations.

Parameter	Symbol	Best estimate
Persistent motion for cells		
Persistence strength infected cells	PS _i	82.43
Persistence strength target cells	PS _t	152.07
Direction update interval infected cells	DT _i	83.66
Direction update interval target cells	DT _t	54.13
Collagen		
Resistance to compression	$\lambda_{Area,C}$	205.28
Membrane stiffness	$\lambda_{Perimeter,C}$	143.18
Adhesion energy		
Energy between target cells	J _{TT}	386.74
Energy between infected cells	J _{II}	91.13
Energy between target and infected cells	J _{TI}	299.59
Energy between target cells and medium	J _{TM}	326.81
Energy between target cells and medium	J _{IM}	341.05
Energy between target cells and collagen	J _{TC}	369.87
Energy between infected cells and collagen	J _{IC}	432.79
CPM		

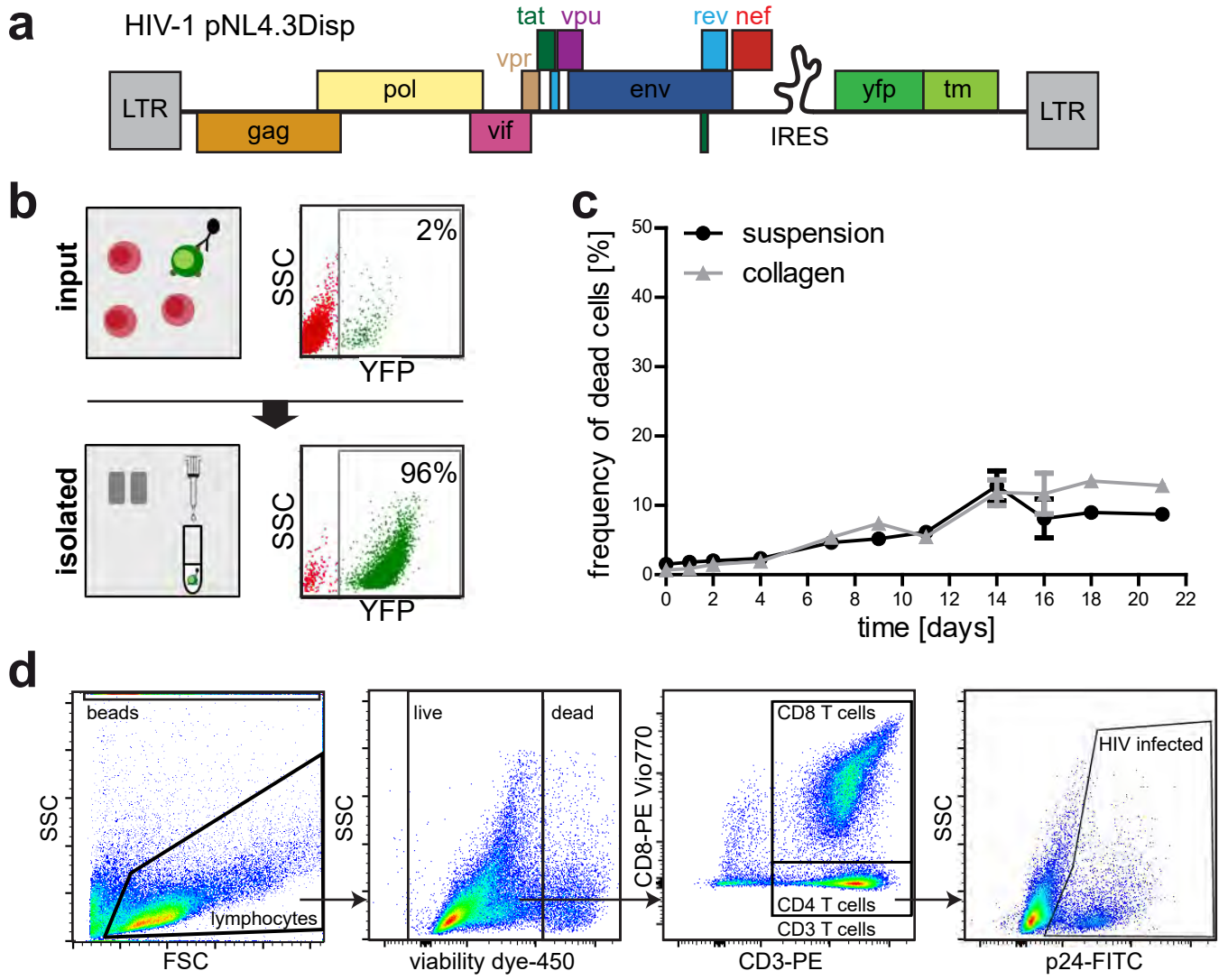
Parameter	Symbol	Best estimate
Temperature	Temp	61.89

20
21
22
23
24
25
26
27
28
29

Supplementary Table 2: Initial number of cells and carrying capacity assumed for different concentrations of cells at the beginning. The carrying capacity C is determined based on the total initial cell number, N , and the assumed relationship $C(N) = C_{max}(1 - e^{-\lambda N})$. The parameter λ was estimated using the observed 4-fold increase for the standard concentration, $C(300)=1200$ cells, the assumption that for lower cell numbers only their proliferative capacity will determine the capacity, leading to $C(150)=600$ cells, and that for a 10-fold higher initial concentration cell growth is limited by the available space in the cell culture, i.e., leading to $C(3000)=4000$ cells.

Cell Type	1x	2x	5x	10x
CD4 uninfected	205	419	1067	2147
CD4 refractory	23	46	118	238
CD4 infected	15	15	15	15
CD8	57	120	300	600
Carrying capacity, C	1200	2021	3367	4000

30

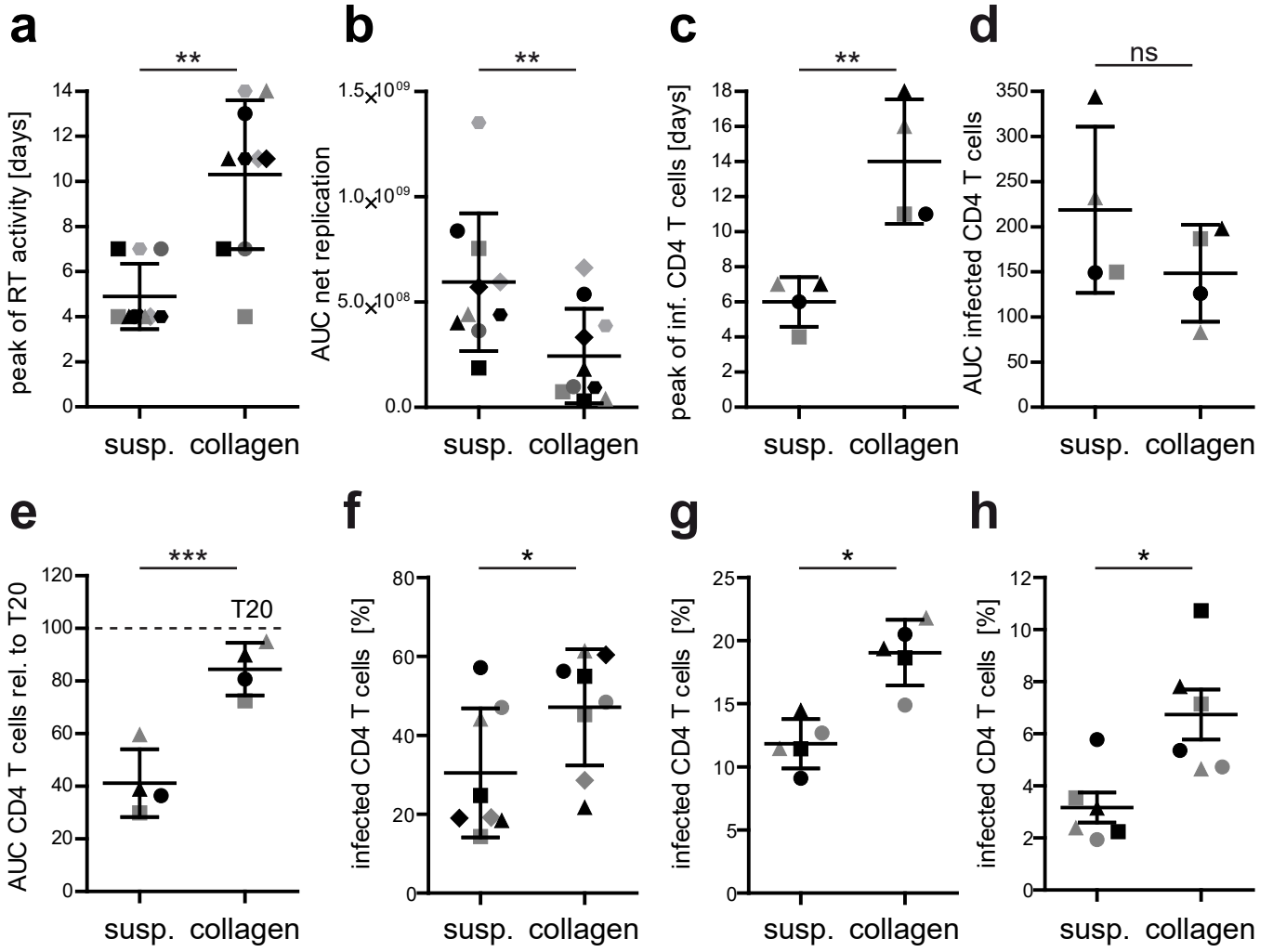


Imle et al. 2018 Supplementary Figure 1

1 **Supplementary Figure 1. Sorting, and gating strategy.**

2 (a) Scheme of sortable provirus (HIV-1 NL4.3 IRES.Display.YFP, HIV-1 NL4.3DispYFP). (b)
3 Principle of purification of infected cells (green). Surface displayed YFP is detected by antibody-
4 coupled magnetic beads, which enable purification by passage through magnetic column. Percentages
5 indicate cell frequency in the respective gate. (c) Viability of lymphocytes in suspension and collagen
6 over time. Fixable viability dye marks dead lymphocytes at indicated time points. The Fig. shows data
7 from one representative out of 4 donors. Mean and standard deviation of triplicate measurement are
8 shown. (d) Gating strategy. From left to right: lymphocyte gate and bead gate for absolute cell
9 quantification displayed among all events. Lymphocytes are distinguished between dead and alive
10 using a fixable viability dye. Live lymphocytes are categorized as CD3 T cells, which are further
11 subdivided in CD8 T cells (CD3+, CD8+) and CD4 T cells (CD3+, CD8-). HIV-1 infected CD4 T
12 cells are detected by anti p24-antibodies.

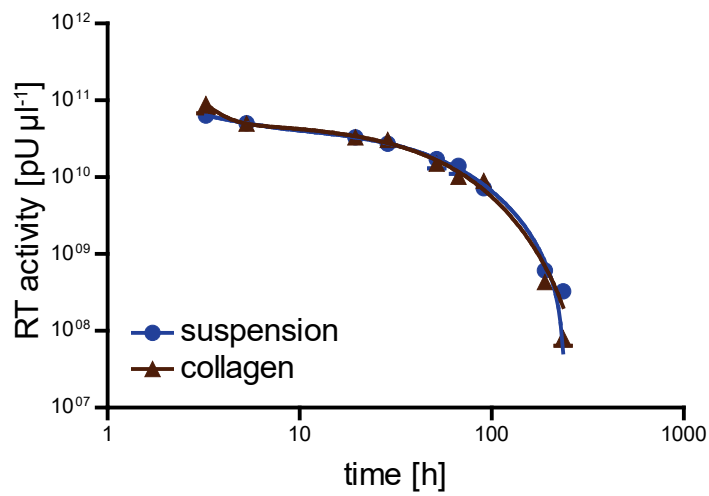
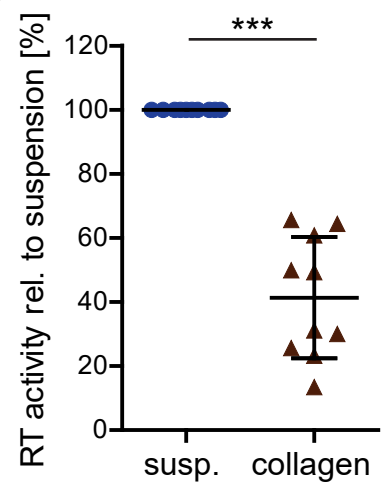
13



Imle et al. 2018 Supplementary Figure 2

14 **Supplementary Figure 2. HIV-1 spread kinetics and permissivity to infection.**

15 HIV-1 spread in suspension or collagen from multiple donors. (a) Day of maximum virus concentration
16 obtained in cells from multiple donors designated by symbol and color. (b) Summary of virus
17 concentration obtained in cells from multiple donors. To monitor net replication, area under the curve
18 values (AUC) of virus concentration in supernatants of T20-treated cultures over 16 up to 21 days
19 were subtracted from AUC values of the corresponding T20-negative samples. (c) Day of maximum
20 percentage of infected CD4 T cells. (d) AUC of percentage of infected CD4 T cells. (e) AUC of
21 residual CD4 T cells relative to respective T20, which was set to 100 (dashed line). Individual points
22 indicate independent experiments using cells from individual donors. Statistical comparisons were
23 based on paired t-test (f-h). (f) Permissivity after culture by cell-free infection. PBMCs were activated
24 and cultured for 4-7 days in suspension or collagen. Subsequently, PBMCs were retrieved from culture
25 by collagenase digestion, counted and spin-infected with HIV-1. After 72 h post infection, infected
26 CD4 cells were quantified by p24-staining in flow cytometry. Individual data points represent means
27 of duplicate to triplicate measurements from independent experiments with different donors. Mean +/-
28 standard deviation, paired t-test. (g) Permissivity after culture by cell-cell infection. PBMCs were
29 activated and either cultured in suspension or collagen. After 72 h, PBMCs were retrieved from
30 suspension and collagen culture by collagenase digestion and counted. For subsequent cell-cell
31 infection, cells were mixed 4:1 with donor-matched PBMCs which had been infected with HIV-1 for
32 72 h (stained with 5 μ M CMTMR). Another 72 h later, infection of CMTMR-negative cells was
33 analyzed by p24-staining in flow cytometry. Mean +/- standard deviation, paired t-test. (h)
34 Permissivity in suspension and collagen culture by cell-free infection. Activated PBMCs were mixed
35 at a MOI of 0.5 with single-round HIV-1 (env pseudotyped pNL4.3 Δ env) and incorporated into
36 suspension or collagen. After 72 h, cells were retrieved by collagenase digestion, and infected CD4
37 cells were quantified by p24-staining in flow cytometry. Mean +/- standard deviation, paired t-test. ns:
38 not significant; *: p-value<0.05; **: p-value<0.01; ***: p-value<0.001.

a**b**

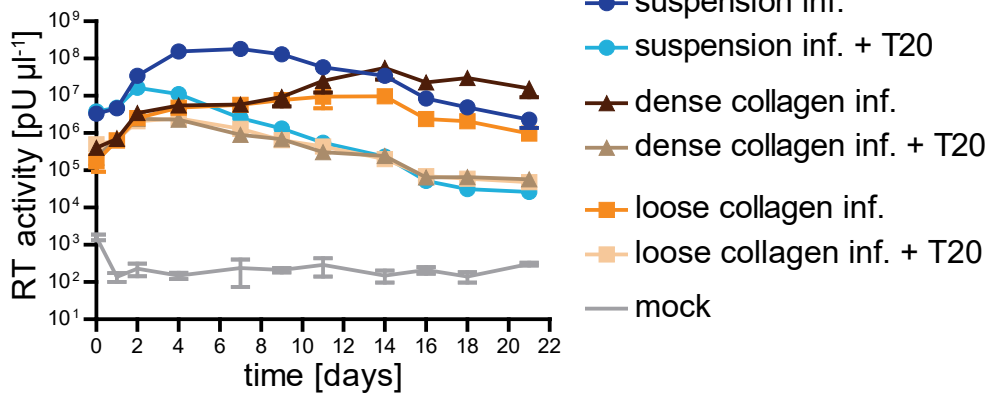
Imle et al. 2018 Supplementary Figure 3

39 **Supplementary Figure 3. Collagen reduces virus production.**

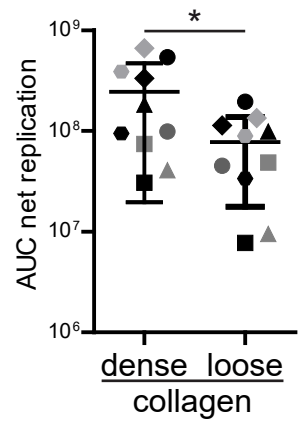
40 (a) Half-time of RT activity for virus embedded in medium (suspension, blue) or collagen (brown). At
41 the indicated time points, total RT activity was quantified as the sum of virus in the supernatant and
42 within the gel (upon collagenase digestion). A two phase decay exponential fit was used to model the
43 data to account for fast decay of free RT from damaged particles and slow decay of RT from intact
44 particles. One representative experiment out of three is shown. Data points indicate mean +/- standard
45 deviation of slow halftimes from the three experiments. (b) Virus production in culture. 72 h upon
46 spin-infection, HIV-1-infected PBMCs were incorporated into suspension or collagen in the presence
47 of 100 μ M T20 to inhibit further spread to target cells. Total virus production was quantified as the
48 sum of SG-PERT signal from supernatants and collagenase digested cultures another 48-72 h later.
49 Data were normalized relative to the results from the respective suspension experiment, which is set
50 to 100%. Individual symbols indicate independent experiments with cells from individual donors.
51 Mean +/- standard deviation, paired t-test was used for statistical analysis.

52

a virus titer supernatant



b

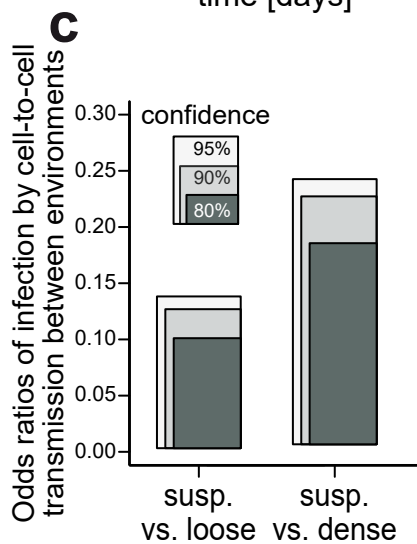
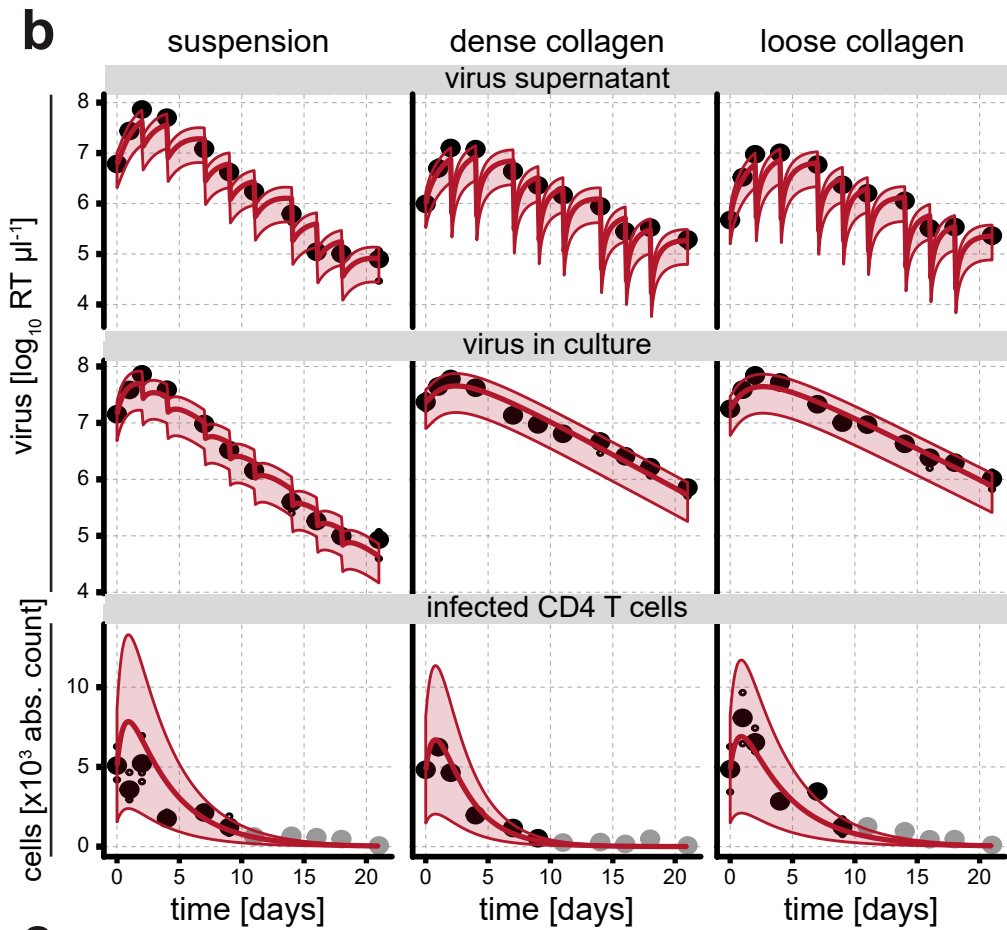
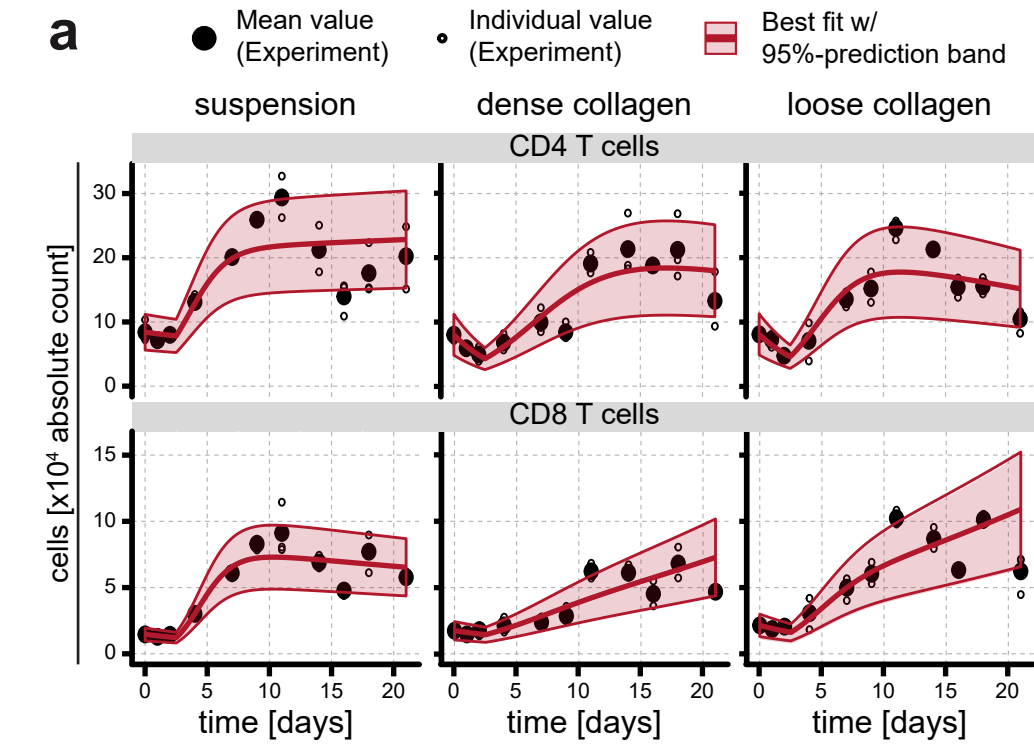


Imle et al. 2018 Supplementary Figure 4

53 **Supplementary Figure 4. 3D confinement dictates HIV-1 spread efficiency**

54 (a) Cells from a representative donor showing HIV-1 spread in suspension, dense and loose collagen
55 over time including respective T20 controls and mock. Virus titers determined from supernatants by
56 SG-PERT. Mean and standard deviation from triplicate measurements are shown. (b) Summary of
57 virus titers obtained in cells from multiple donors designated by color and symbol. To monitor net
58 replication, AUC values of virus concentration in supernatants of T20-treated cultures over 16 up to
59 21 days were subtracted from AUC values of the corresponding T20-negative samples. Individual
60 points indicate independent experiments with cells from individual donors. Paired t-test was used for
61 statistical analysis.

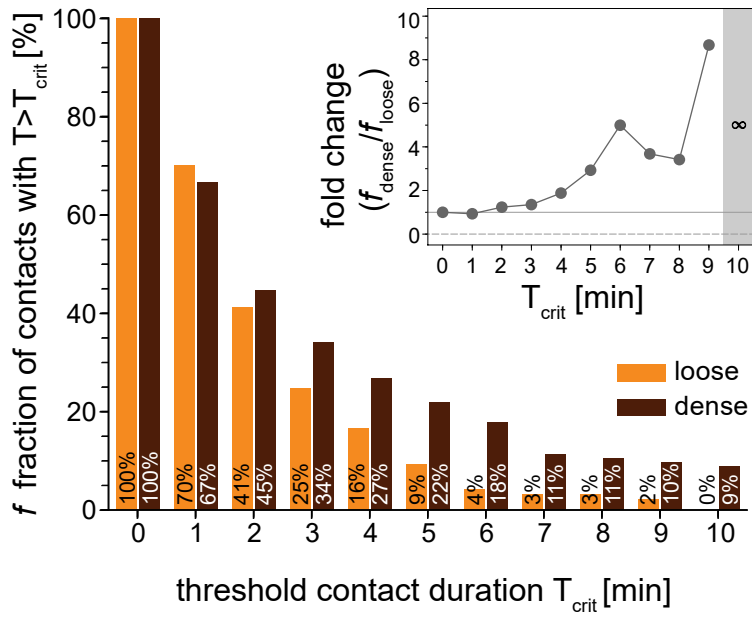
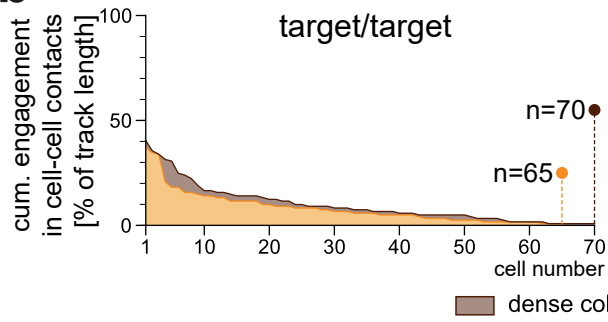
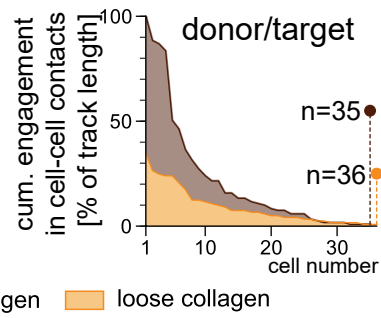
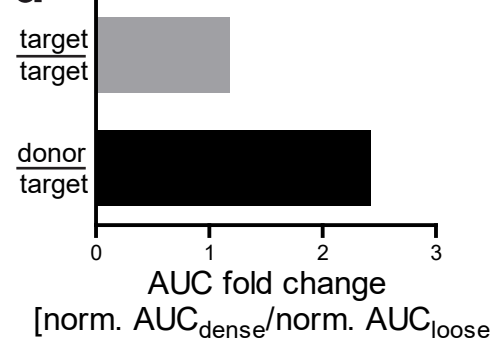
62



63 **Supplementary Figure 5. Modelling of cell proliferation and viral turnover.**

64 (a) Modelling of absolute count data of CD4 and CD8 T cells to determine proliferation parameters.
65 (b) Modelling of virus kinetics in T20 treated samples to determine virus production and infected cell
66 life span. (c) Odds-ratios for infection by cell-to-cell transmission between suspension and loose (left)
67 and suspension and dense (right) collagen based on the obtained parameter estimates for β_c and β_f
68 (Table 1, Fig. 3e). The odds for each environment define the chance of infection by cell-to-cell
69 transmission (P_{CC}) vs. infection by cell-free infection (P_{CF}) in this particular environment ($O=P_{CC}/P_{CF}$).
70 The ratio between the odds for two different environments (e.g., $OR_{SL}=O_S/O_L$) then provides an
71 estimate of how much more likely it is to be infected by cell-to-cell transmission in the one
72 environment compared to the other. For example, an odds ratio of $O_{SD}=0.25$ as observed between
73 suspension (S) and dense (D) collagen indicates that the chance of a cell being infected by cell-to-cell
74 transmission is 4-times more likely in dense collagen compared to suspension. Gray-shaded areas
75 indicate the different levels of confidence for parameter estimates.

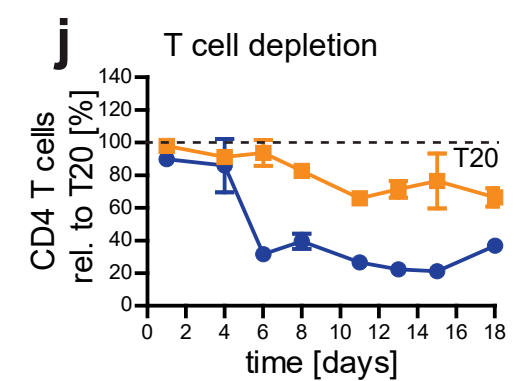
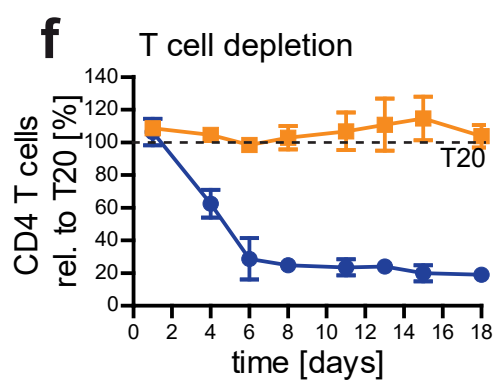
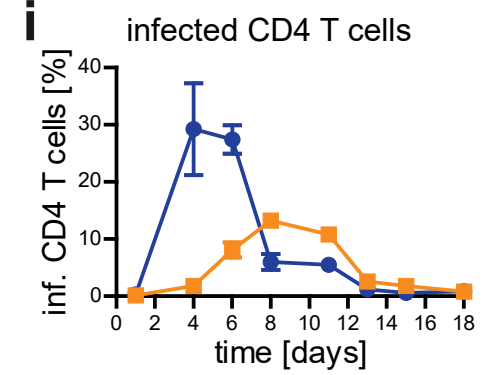
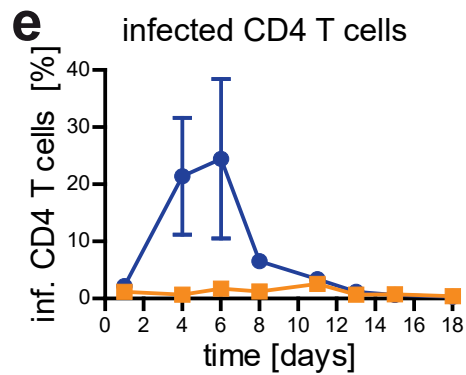
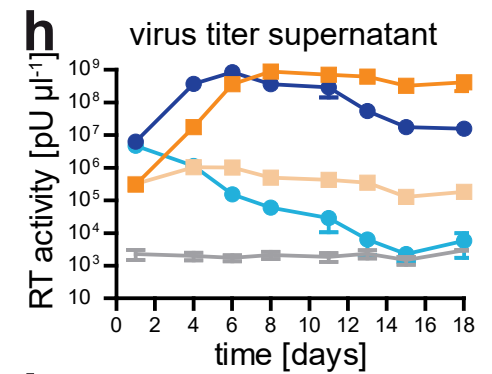
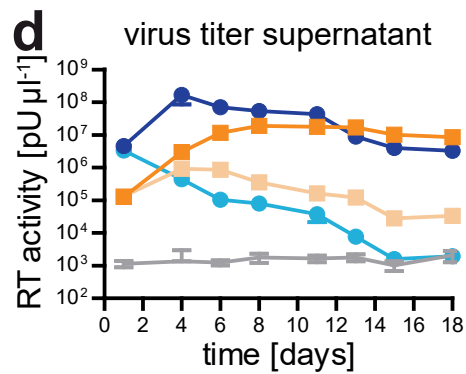
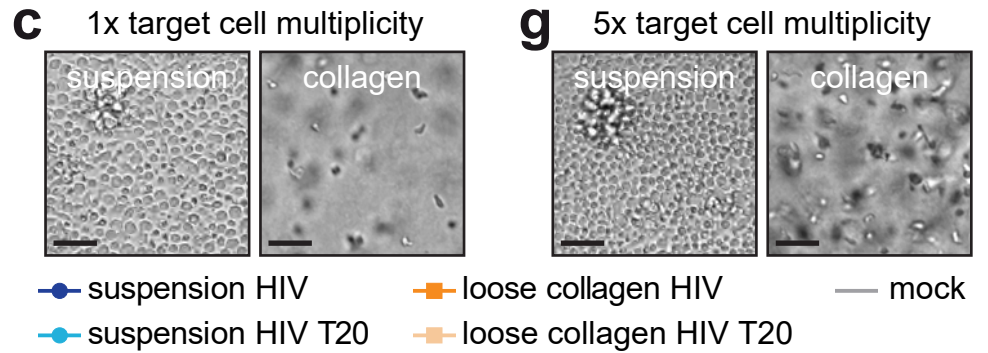
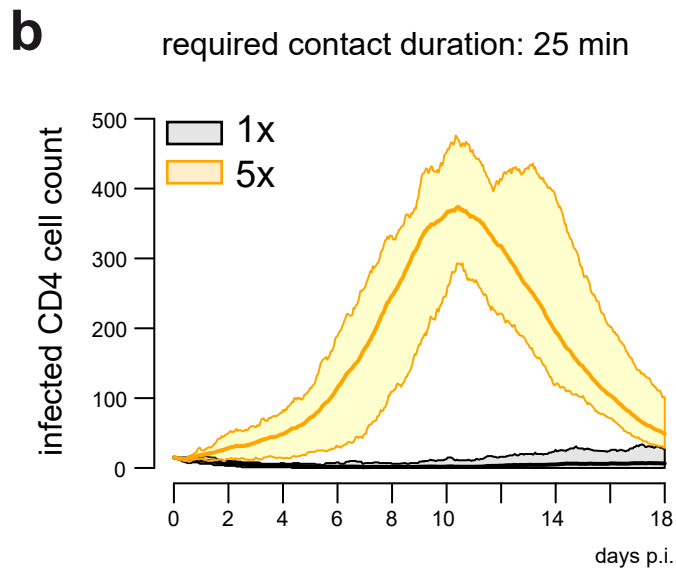
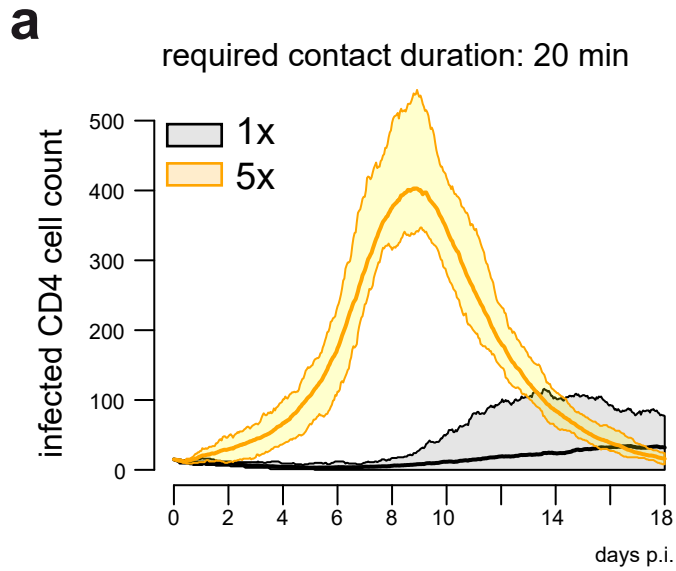
76

a**b****c****d**

77 **Supplementary Figure 6. Advanced contact analysis.**

78 (a) Fraction of cell-cell contacts exceeding a critical threshold contact duration T_{crit} for infected
79 cell/target cell pairs. The inset shows the fold change between fraction of contacts between dense and
80 loose collagen. (b) Cumulated target-target cell contact duration normalized to the full track duration,
81 which is set to 100%. Brown and ochre curves depict contacts in dense and loose collagen,
82 respectively, indicating the number of cells displaying the indicated cumulative contact duration. n
83 indicates the total amount of tracks analyzed. (c) Cumulated donor-target cell contact duration
84 displayed as in (b). (d) The difference between cumulated contacts for target/target and donor/target
85 contacts as shown in (b) and (c) was computed as the ratio between areas under the curve (AUC) for
86 dense and loose collagen normalized to the amount of tracks.

87



88 **Supplementary Figure 7. CPM simulation with increased target cell concentrations confirm**
89 **minimal contact duration for productive HIV-1 spread via cell-to-cell transmission.**

90 (a, b) Simulated infection dynamics based on the CPM using the standard (1x, black) or five-fold
91 higher (5x, orange) concentration of target cells assuming either that a contact duration of 20 (a) or 25
92 (b) minutes between infected and uninfected cells is necessary for cell-to-cell spread. The mean (solid
93 lines) and the minimal and maximal number of infected cells per time point (shaded area) over 10
94 independent simulations per concentration are shown. (c-j) Experimental data including T20 and mock
95 control for comparison of the infection dynamics in suspension (blue) and loose collagen (orange)
96 using the standard (1x, c-f) and 5-fold increased (g-j) concentration of target cells. Scale bar of
97 representative bright field images: 40 μ m. (d, h) Virus titers determined from supernatants by SG-
98 PERT. (e, i) Percentage of infected (p24+) CD4 T cells determined by FACS. (f, j) T cell depletion
99 expressed as residual CD4 T cells relative to respective T20 control, which was set to 100% (dashed
100 line). Mean values and standard deviations from triplicate measurement are shown.

101